



Extreme rainfall trends of 21 typical urban areas in China during 1998–2015 based on remotely sensed data sets

Weiyue Li · Min Zhao · Marco Scaioni ·
Seyed Reza Hosseini · Xiang Wang · Dongjing Yao ·
Kaihang Zhang · Jun Gao · Xin Li

Received: 21 May 2019 / Accepted: 17 October 2019 / Published online: 1 November 2019
© Springer Nature Switzerland AG 2019

Abstract With the increase of population, many cities are growing in size at a phenomenal rate. Urbanization changes the urban underlying surface, influences the micro-climate, and sometimes affects the local precipitation process. In this study, we investigated the trends of extreme rainfall in China's 21 typical urban areas. Based on a series of daily rainfall and "Urban/built-up" dataset from TMPA 3B42 and MCD12Q1 products in China, trends in extreme precipitation, with the threshold defined as 95th (pre95p) and 99th (pre99p) percentiles of annual rain days during 1998–2015, have been assessed in China, and especially in 21 typical urban areas from 1998 to 2015. The tendency curves in ex-

treme rainfall of different years are presented. In this period, more than 66% regions of China covered by TMPA 3B42 have increasing trends in extreme rainfall with pre95p threshold. The 21 typical urban areas showed different trends—in over half of these areas, upward tendencies in extreme rainfall were observed, particularly in Dalian, Beijing, and Chongqing. Seventeen urban areas showed increasing tendencies in pre95p extreme rainfall days, including Shanghai, Nanjing, Hangzhou, and Suzhou in the Yangtze River Delta region. The results also illustrate that southeastern coastal urban areas of China may have experienced decreasing occurrences in extreme rainfall.

W. Li · J. Gao
Institute of Urban Studies, Shanghai Normal University,
Shanghai 200234, China

W. Li · D. Yao · J. Gao
School of Environmental and Geographical Sciences, Shanghai
Normal University, Shanghai 200234, China

W. Li · M. Zhao (✉)
Shandong Provincial Key Laboratory of Water and Soil
Conservation and Environmental Protection, College of Resources
and Environment, Linyi 276005, China
e-mail: zmm720@163.com

M. Scaioni
Department of Architecture, Built Environment and Construction
Engineering, Politecnico di Milano, 20133 Milan, Italy

S. R. Hosseini
Department of Civil and Environmental Engineering, Politecnico
di Milano, 20133 Milan, Italy

X. Wang
Linyi Natural Resources and Planning Bureau, Linyi 276001,
China

K. Zhang
Institute of Tourism, Shanghai Normal University,
Shanghai 200234, China

X. Li
Institute of Tibetan Plateau Research, Chinese Academy of
Sciences, Beijing 100101, China

X. Li
CAS Center for Excellence in Tibetan Plateau Earth Sciences,
Chinese Academy of Sciences, Beijing 100101, China

Keywords Extreme rainfall trends · Rainfall threshold · Urban areas · Satellite-based precipitation · Remotely sensed data

Introduction

Variations in the spatiotemporal distribution of both global and regional precipitations are among the most relevant aspects of climate change in a globally warming world (Donat et al. 2016). Rainfall events may sometimes occur with particularly strong intensity, to be referred to as rainfall extremes, which are frequently responsible for natural hazards such as flash floods, landslides, and debris flows (Aalst 2006; Barredo 2007; IPCC 2013; Pendergrass and Knutti 2018). Recent Intergovernmental Panel on Climate Change (IPCC) reports show that the frequency of extreme rainfall events has generally increased with global climate warming and elevated atmospheric CO₂ concentrations (Allan and Soden 2008; O’Gorman 2015). Some studies indicate that global temperature difference between day and night presents a downward trend, but annual rainfall and rainfall extremes have been rising since the beginning of the twentieth century (Alexander et al. 2012; Chou et al. 2012). Especially in the middle and high latitudes of northern Hemisphere, average daily rainfall has gradually decreased in some regions, where an upward trend of rainfall extremes can be observed as well because snow-cover extent loss favors descending air motion (Tang et al. 2014). Additionally, some climate models show that the above trends would keep growing under the current greenhouse conditions influenced by human activities (Meehl et al. 2005; Tebaldi and Knutti 2007).

One important aspect about the observed intensification of extreme rainfall events concerns urban areas. Since the urban atmospheric boundary layer and local climatic environment are affected by human activities and the underlying surface, more extreme rainfall events have been recorded over urban areas compared with suburbs (Georgescu et al. 2014). The main reason is that the number of clouds in urban areas is obviously higher than that in suburbs. This phenomenon depends upon three main factors: (1) urban-heat-island effect (Rajasekar and Weng 2009) that frequently causes local air rising and forms clouds (Agarwal and Tandon 2010); (2) more cloud condensation nuclei from anthropogenic greenhouse gases suspends in the urban air (Ackerman et al.

2004); and (3) friction effect from urban underlying surface that makes clouds move slowly in urban areas, while buildings force local air rising up (Han et al. 2014). More clouds over cities increase the occurrences of rainfall, especially the extreme ones. More than half of the world’s population now lives in urban areas, and urban hazards caused by extreme rainfall frequently follow the urban expansion observed in recent years.

The scenario described above has been analyzed in this study by considering China as a case study. In China, the problem of extreme rainfall is of paramount relevance because of the large number of inhabited areas and the huge number of cities and megacities. In addition, some urban areas in the east and south of the country are also vulnerable to floods triggered by extreme rainfall events (Wang et al. 2013; Quan 2014; Yang et al. 2015).

Changes of extreme rainfall in China show clear regional differences (Zhai et al. 1999), since different trends have been observed from ground meteorological stations (Qian and Lin 2005; Zhai et al. 2005; Wang and Yan 2009). Some cities, such as Shanghai, Nanjing, and Guangzhou, show rain-island characteristics (Liang et al. 2013; Hu et al. 2016; Chen et al. 2016). However, studies carried out so far are limited in their scope and they did not fully exploit the potential of currently available data sets. The standard method adopted for rainfall monitoring is based on ground meteorological stations that, however, are not evenly distributed over the Chinese territory. For example, well-developed and highly inhabited regions have more meteorological stations in eastern than western China, while some regions may completely lack any station to record real-time precipitation changes. Even in a dense rain gauge network, the uneven spatial distribution of the stations and the complex orography may reduce the chances of observing precipitations (Libertino et al. 2016). Additionally, due to the small spatial extension of urban areas, this type of extreme rainfall sometimes may be difficult to sample by using sparse ground meteorological stations. Thus, remote sensing data may be a way to estimate the spatiotemporal features over the whole precipitation field (Olson et al. 1996).

Satellite-based precipitation estimation has witnessed significant developments in recent years (Joyce et al. 2004; Huffman et al. 2007; Chen et al. 2013; Sorooshian et al. 2000). The rate of rain modeling can be derived using GIS from remote sensing data. Recently, some studies showed that one of the climatic factors is rain (Cetin 2015a, b; Cetin and Sevik 2016; Yucedag et al.

2018). Modeling remote sensing is useful to determine rainfall (Cetin 2015a, b, 2016). Recent studies show that global warming changes are explained by remote sensing, focusing on the sustainability assessment of ecosystem linkage. Scenarios with high-quality remote sensing have been developed. Monitoring provides consistent and comprehensive information to complement management and ground-based information (Kaya et al. 2018; Cetin et al. 2018). Among the available products, gauge-corrected Tropical Rainfall Measuring Mission (TRMM) Multi-satellite Precipitation (TMPA)¹ is one of the most widely used quasi-global post-real-time products. The primary-merged microwave-infrared product is computed at a 3-h temporal resolution (TMPA 3B42) and $0.25^\circ \times 0.25^\circ$ spatial resolution. The latest version 7² is a gauge-adjusted real-time TRMM product covering the 1998–present period derived from observations from various satellite systems. The product can greatly benefit the detection and the evaluation of extreme rainfall events, flash flooding, and landslides (Chen et al. 2013; Tarnavsky et al. 2013; Li et al. 2017a, b). Some studies have proved that TRMM version 7 product can indicate the real rainfall spatio-temporal distribution, having a higher correlation with observations from rainfall gauges in different regions of China (Xu et al. 2009; Huang et al. 2010; Jia et al. 2011; Huang et al. 2013).

In this study, TMPA 3B42 products were used to analyze daily extreme rainfall trends of 21 typical urban areas and to obtain their temporal variations and spatial distributions over the period from 1998 to 2015.

Data, study area, and methods

In this section, we first make a brief introduction to the remote sensing data preparation, study area, and proposed methods.

Data preparation

This study used two kinds of data from remotely sensed product. The first is the rainfall data from TMPA 3B42 product, available at the TRMM website. The product covers the region between latitude 50°N and 50°S and

¹ <http://trmm.gsfc.nasa.gov>

² https://mirador.gsfc.nasa.gov/collections/TRMM_3B42_daily_007.shtml

longitude 180°W and 180°E (Huffman et al. 2007). For this study, a data set of daily rainfall spanning over years 1998–2015 was downloaded.

The second is the “Urban/built-up” data from MCD12Q1, TM, and ETM products. MCD12Q1 is a level 3/level 4 product of the Moderate Resolution Imaging Spectroradiometer (MODIS) land cover data sets and has a 500-m resolution (Pfeifer et al. 2011). This product that can be obtained from the MODIS website³ based on the processing of yearly observations from Terra and Aqua satellites and can be applied to classify land cover types in 2001–2013. MCD12Q1 product consists of five land cover classification systems. In this study, the International Geosphere-Biosphere Programme (IGBP) global vegetation classification scheme (Zhang et al. 2018) was chosen, including 17 land cover types. The scheme is currently considered the best primary data source of global land cover class information (Zeng et al. 2016). Type “Urban/built-up” is used to represent anthropogenic urban areas.

Unfortunately, MCD12Q1 product cannot cover the years 1998, 1999, 2000, 2014, and 2015. We obtained another free product, TM/ETM+, from the website (<http://glovis.usgs.gov/>) of U.S. Geological Survey (USGS). Based on the classification of MCD12Q1, we extracted the urban areas then resized the classification results into 500 m resolution to be the same with MCD12Q1.

Study area

With rapid urbanization in the last 30 years, the urbanization rate of Eastern China is close to the level of developed countries (Yang 2013). We selected the typical 21 urban areas in Eastern China, including Beijing, Tianjin, Shenyang, Dalian, Jinan, Qingdao, Zhengzhou, Xi’an, Chengdu, Chongqing, Changsha, Wuhan, Nanjing, Suzhou, Shanghai, Hangzhou, Guangzhou, Shenzhen, Xiamen, Fuzhou, and Taipei (Fig. 1), where nearly 250 million people reside. We further divided the 21 typical urban areas into four study regions including northeastern China and North China, southwestern and central China, the Yangtze River Delta region, and southeastern and southern China, as shown in Fig. 1. We chose type “Urban/built-up” from MCD12Q1 products as

³ <https://modis.gsfc.nasa.gov/>

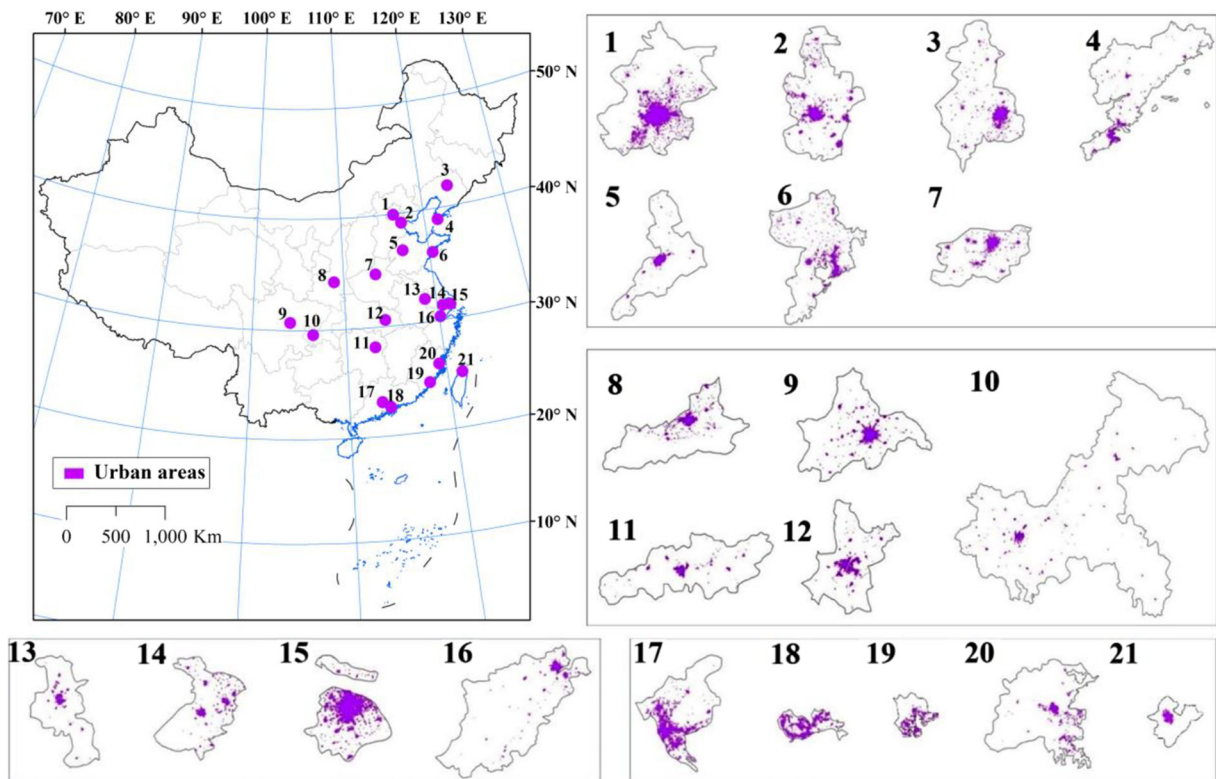


Fig. 1 Spatial distribution of the 21 typical urban areas in 2015. (1) Beijing. (2) Tianjin. (3) Shenyang. (4) Dalian. (5) Jinan. (6) Qingdao. (7) Zhengzhou. (8) Xi'an. (9) Chengdu. (10) Chongqing.

(11) Changsha. (12) Wuhan. (13) Nanjing. (14) Suzhou. (15) Shanghai. (16) Hangzhou. (17) Guangzhou. (18) Shenzhen. (19) Xiamen. (20) Fuzhou. (21) Taipei

urban areas combining with the data from the land use classification results in 2015.⁴

Analysis techniques and background

In China, heavy rainfall and severe rainstorm are considered as extremes when daily rainfall amounts reach above 50 mm and 100 mm, respectively (Domrös and Peng 2012). Extreme rainfall may cause a variety of damage and the criteria have been used by researchers and officials as indicators to estimate and simulate the potential urban flooding. However, in most regions of China, rainfall extremes greater than 50 mm are very rare. Particularly in the western arid region of China, even heavy rainfall events are very rare due to lack of rainfall. Figure 1 shows some typical urban areas located in the middle or the midwest. Therefore, we defined the relative extreme rainfall events with daily rainfall amount greater than the 95th and 99th percentiles of annual rain days during 1998–

2015. In other words, the threshold accounts for 95th and 99th percentiles of all daily rainfall amounts in 1 year. The method of determining extreme precipitation threshold has been widely explored in recent studies (e.g., Frich et al. 2002; Zhai et al. 2005; Wu et al. 2015).

In order to analyze the trend within time of extreme rainfall, a linear model has been used to fit rainfall data:

$$y(t) = b + a \cdot t \quad (1)$$

where t is the time; $y(t)$ is the variable indicating the extreme rainfall. The parameters a and b are the regression intercept and coefficient, respectively. The value of a represents the estimated rate of the extreme rainfall changes, while its sign shows whether these are undergoing a growth or a decrease. In addition, the estimated changes of rainfall (ECsR, mm) between t_n and t_1 can be calculated by Eq. 2.

$$ECsR = \frac{\sum_{t=1}^n [y(t+1) - y(t)]}{n-1}, \quad n > 1 \quad (2)$$

⁴ <https://climatedataguide.ucar.edu/climate-data/ceres-igbp-land-classification>

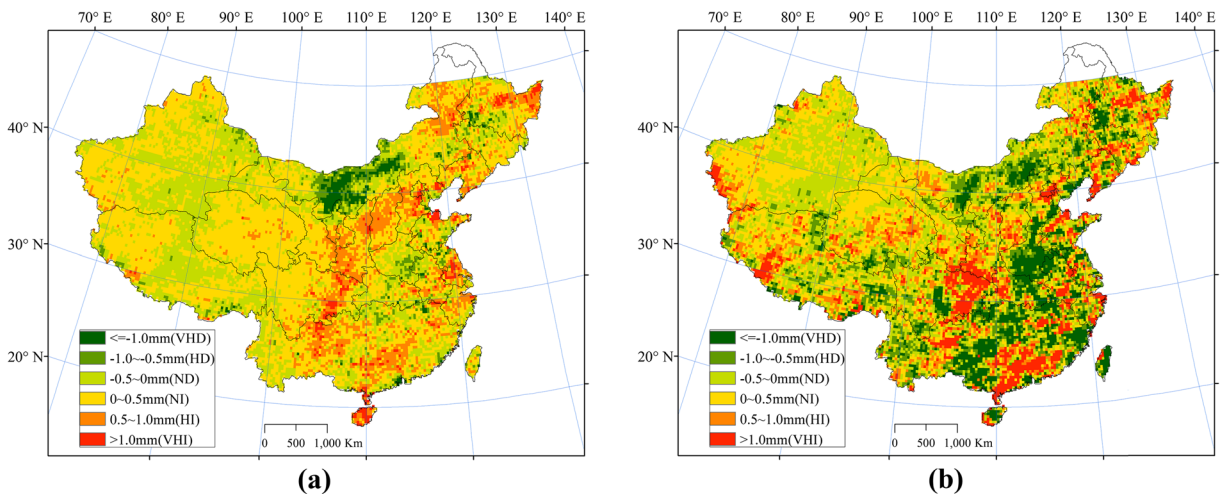


Fig. 2 Trend distributions of extreme rainfall from 1998 to 2015. **a** 95th percentile. **b** 99th percentile

To quantify the spatiotemporal changes of daily rainfall in urban areas, the average of daily extreme rainfall in urban area (AD_i) is calculated as follows:

$$AD_i = \frac{\sum_{j=1}^n UP_{i,j}}{\sum_{i=1}^n Num_{i,j}} \quad (3)$$

where $UP_{i,j}$ is the extreme rainfall of the j th grid, and $Num_{i,j}$ is the number of grids having urban areas at city i .

Results on trends of extreme rainfall

This section includes two parts: “Trend distributions of extreme rainfall” shows the results on the trend distributions of extreme rainfall, and “Trends of extreme rainfall in urban areas” describes and analyses the changes of extreme rainfall in 21 typical urban areas from 1998 to 2015.

Trend distributions of extreme rainfall

We used Eq. 1 to fit the trend changes of extreme precipitation from 1998 to 2015 including the 95th percentile (prec95p) and 99th percentile (prec99p), and calculated the ECsR. The values of ECsR are classified into six categories using 0.5 mm as intervals: ≤ -1.0 mm, very high decrease (VHD); $-1.0 \sim -0.5$ mm, high decrease (HD); $-0.5 \sim 0$ mm, normal decrease (ND); $0 \sim 0.5$ mm, normal increase (NI); $0.5 \sim 1.0$ mm, high increase (HI); > 1.0 mm, very high increase (VHI). Figure 2 shows that VHI regions having increasing trends in extreme rainfall are distributed mainly over southern and central regions of mainland China. Especially for prec99p, most of the regions have increasing trends of extreme rainfall in Guangdong and the east of Sichuan. Figure 3 shows the comparisons on proportion of the six categories. More than 66% (50%) of the regions have increasing trends

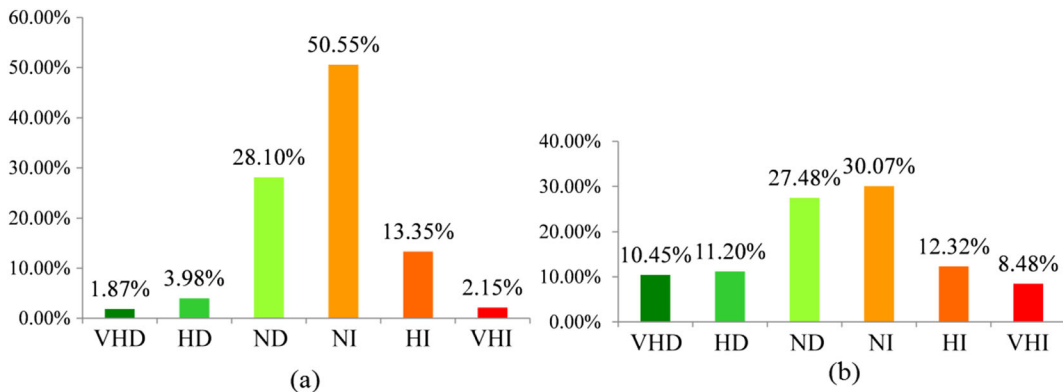


Fig. 3 Comparisons on the proportion of the six categories. **a** prec95p. **b** prec99p

(i.e., NI, HI, and VHI) in pre95p (pre99p) extreme precipitation. It is noted that 8.48% regions may have more than 1.0 mm annual increase in pre99p extreme precipitation during 1998–2015.

applied to find the trends of extreme rainfall indicators (AD_i) in the 21 typical urban areas.

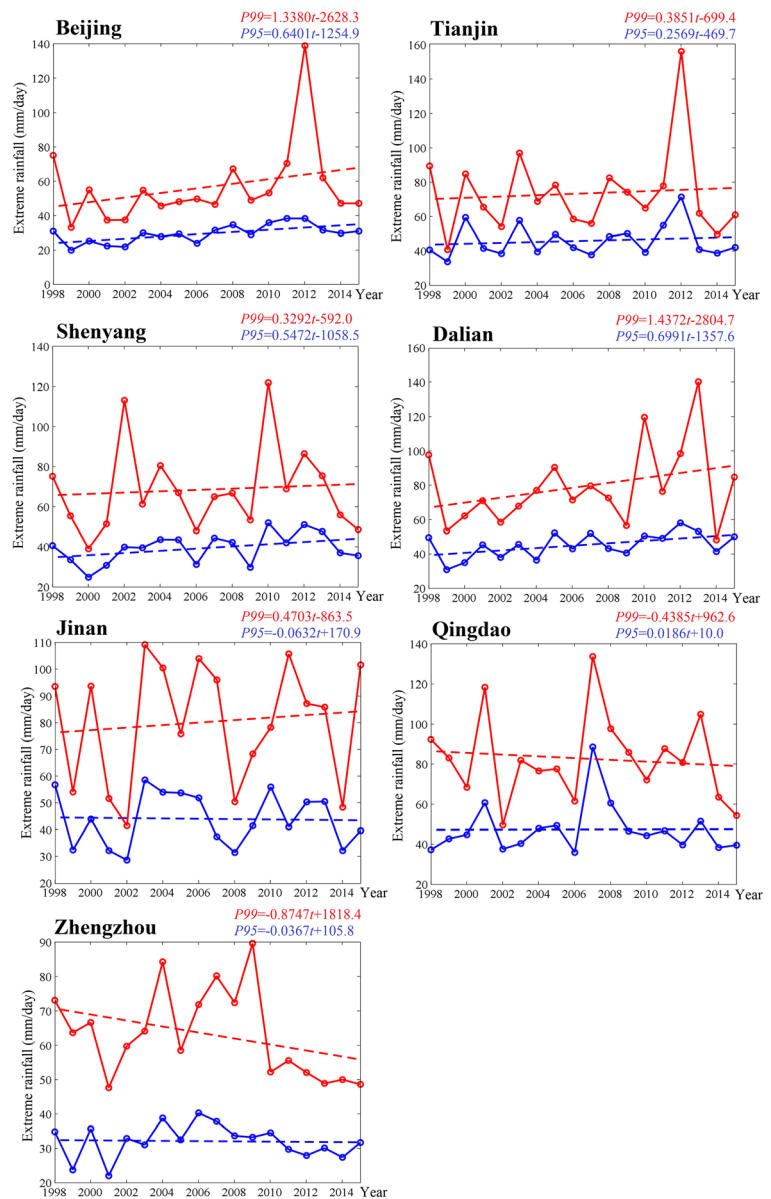
Trends of extreme rainfall in urban areas

Trends of extreme rainfall in urban areas in northeastern China and North China

In “Trend distributions of extreme rainfall,” the distribution of pre95p and pre99p extreme rainfall in China based on the analysis of TMPA 3B42-V7 products in 1998–2015 has been described. In this section, Eq. 3 is

The northeastern part of China and North China feature a wet sub-humid climate. The average annual rainfall amount is between 200 and 800 mm. The trends in prec95p and prec99p are calculated in different urban areas where seven big cities are located in this group:

Fig. 4 Trend of extreme rainfall in the seven urban areas of northeast China and North China



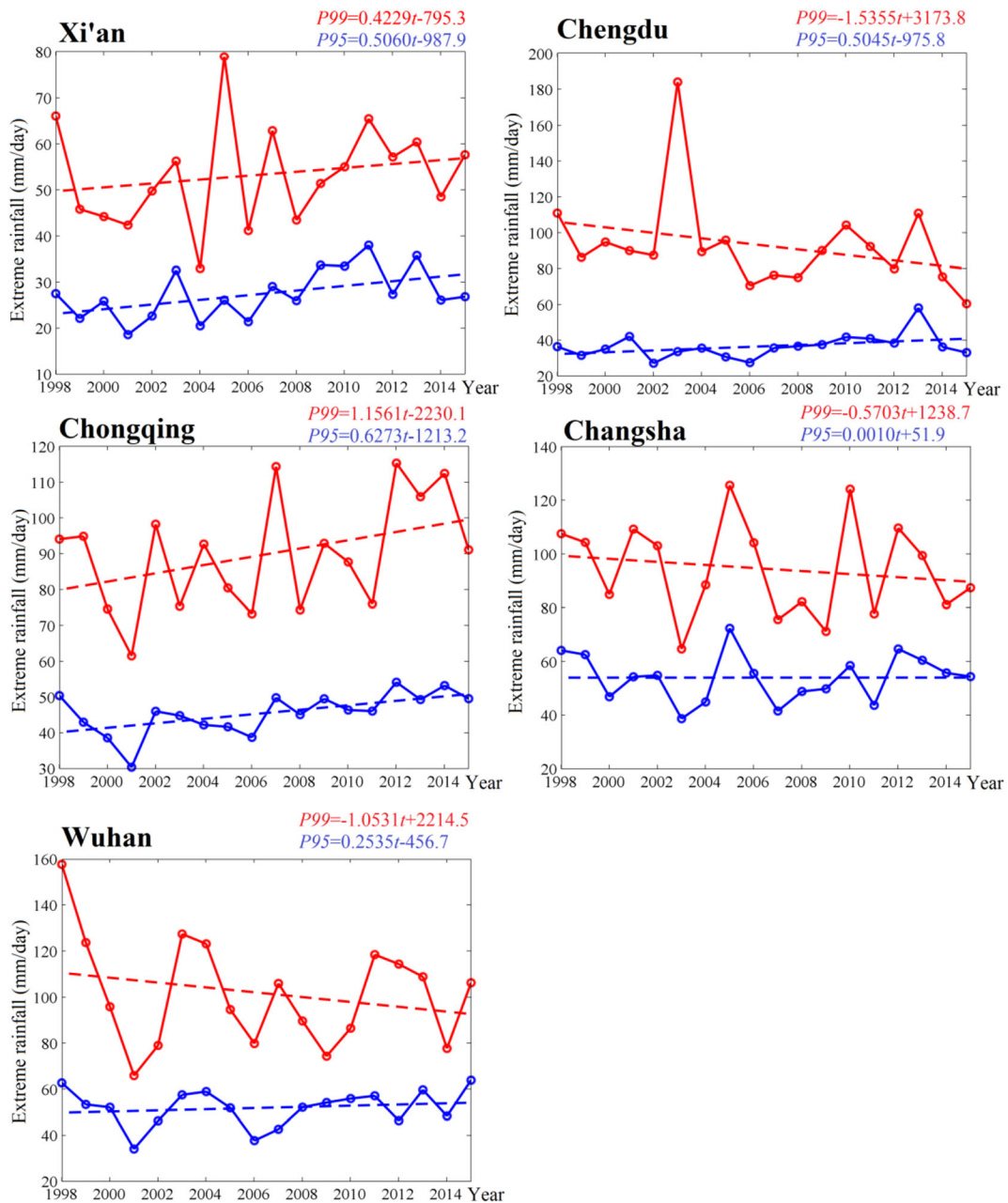


Fig. 5 Trend of extreme rainfall in the five urban areas of southwestern and central China

Beijing, Tianjin, Shenyang, Dalian, Jinan, Qingdao, and Zhengzhou (Fig. 1). In which, $P95$ ($P99$) is estimated $prec95p$ ($pre99p$) extreme daily rainfall based on Eq. 1.

Results of Tianjin show the highest value for $pre99p$ extreme rainfall approaching 160 mm/day in 2012, while the highest value for $pre95p$ extreme rainfall (larger than 80 mm/day) has occurred in Qingdao.

Inversely, Zhengzhou has the lowest $pre95p$ value (lower than 40 mm/day) (see Fig. 4).

The parameter a shows an upward extreme rainfall tendency in Beijing, Tianjin, Shenyang, and Dalian. In particular, Dalian has the fastest increase of $pre95p$ ($|a| = 0.6991$) and $pre99p$ ($|a| = 1.4372$) extreme rainfall. Results of Zhengzhou show a downward extreme rainfall

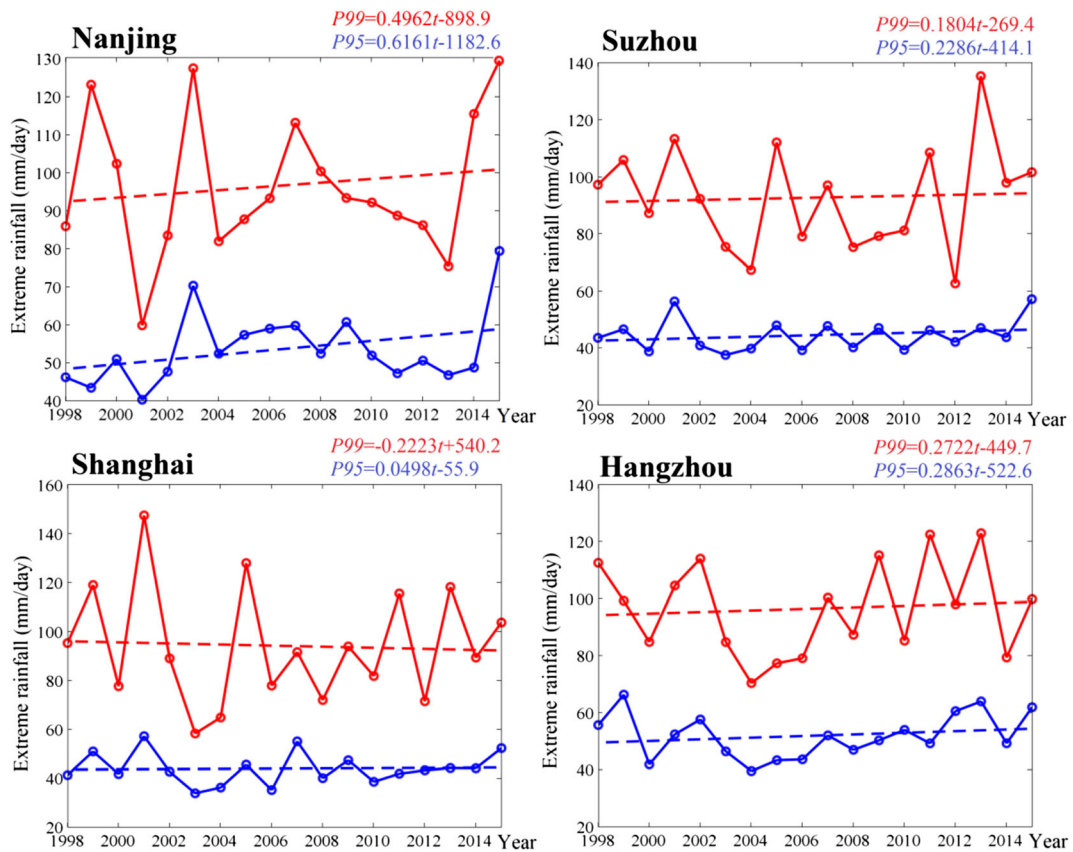


Fig. 6 Trend of extreme rainfall in the four urban areas of Yangtze River Delta region

tendency, especially for pre99p, the value of parameter a is -0.8747 . On the contrary with Qingdao, Jinan has upward tendency of $P99$, while $P95$ has gone downwards.

Trends of extreme rainfall in southwestern and central China

The southwestern and central parts of China also have a wet sub-humid climate similar to northern China. The average annual rainfall is over 400 mm. Five big cities Xi'an, Chengdu, Chongqing, Changsha, and Wuhan are analyzed in this region (Fig. 1).

Results of Chengdu show the highest value for pre99p extreme rainfall larger than 180 mm/day in 2003, while Changsha has the highest value for pre95p extreme rainfall approaching 80 mm/day in 2005. Inversely, Xi'an has the lowest pre95p value (lower than 40 mm/day) (see Fig. 5).

During the period 1998–2015, $P95$ and $P99$ show upward tendencies in Xi'an and Chongqing. In particular, Chongqing has the fastest increase of pre95p ($|a| =$

0.6273) and pre99p ($|a| = 1.1561$) extreme rainfall. Wuhan, Chengdu, and Changsha have upward tendency of $P95$, while $P99$ have gone downwards.

Trends of extreme rainfall in the Yangtze River Delta region

The Yangtze River Delta region has a marine monsoon subtropical climate. The average annual rainfall is over 800 mm. Four big cities—Nanjing, Suzhou, Shanghai, and Hangzhou—are located here, which are the main urban built-up areas of this region (Fig. 1).

Figure 6 shows the temporal changes of pre95p and pre99p extreme rainfalls in the four urban areas. Results of Shanghai show the highest value for pre99p extreme rainfall larger than 140 mm/day in 2001, while Nanjing has the highest value for pre95p extreme rainfall larger than 80 mm/day in 2015.

Except for the pre99p trend in Shanghai, other urban areas have upward tendencies in extreme rainfall during

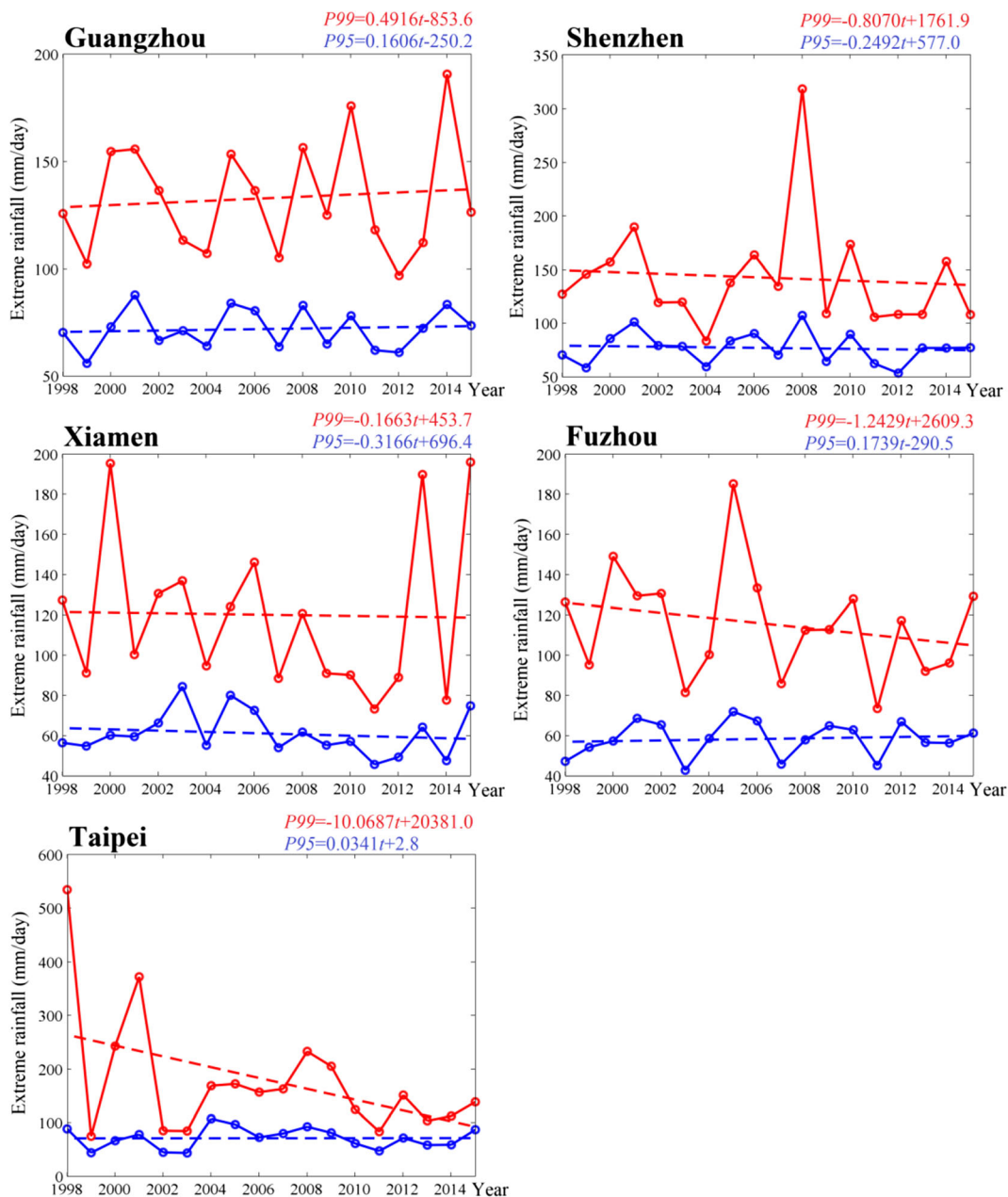


Fig. 7 Trend of extreme rainfall in the five urban areas of southeastern and southern China

1998–2015. Nanjing has the fastest changes of pre95p ($|a| = 0.6161$) and pre99p ($|a| = 0.4962$).

Trends of extreme rainfall in southeastern and southern China

The southeastern and southern parts of China have a wet climate, with an average annual rainfall over 800 mm. Five big cities (Guangzhou, Shenzhen, Xiamen, Fuzhou, and

Taipei) are found in this area (Fig.1), which face high risk of typhoons and the consequent extreme rainfall events.

Figure 7 shows the temporal changes of pre95p and pre99p extreme rainfall in the five urban areas where the daily extreme rainfall is over 40 mm/day during 1998–2015. Results of Taipei show the highest value for pre99p extreme rainfall larger than 500 mm/day in 1998.

During the period 1998–2015, P95 and P99 show upward tendencies in Guangzhou and show downward

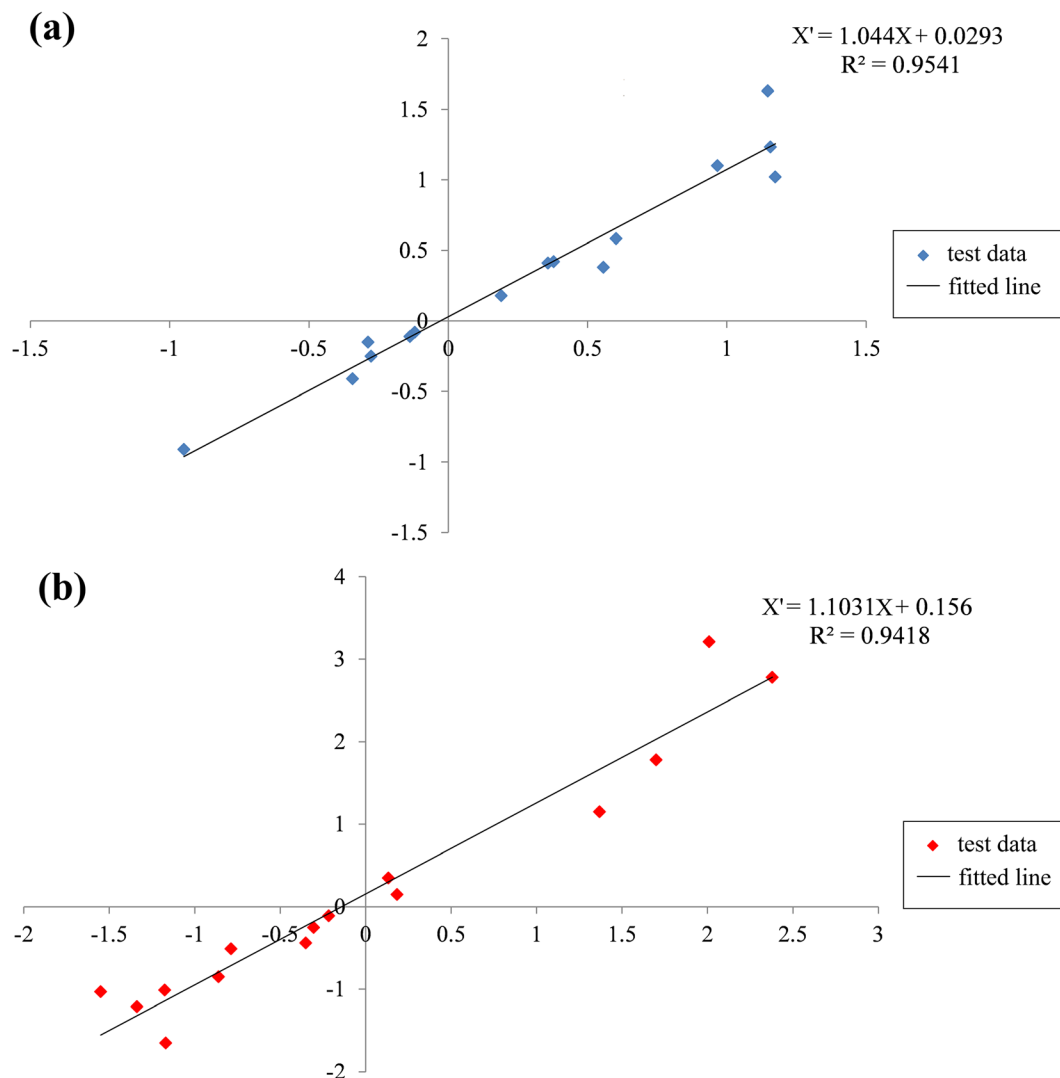


Fig. 8 The trends in pre95p (a) and pre99p (b) extreme rainfall based on TMPA against rain gauges

tendencies in Xiamen and Shenzhen. Xiamen has the fastest changes of pre95p ($|a| = 0.3166$), and Taipei has the fastest pre99p ($|a| = 10.0687$).

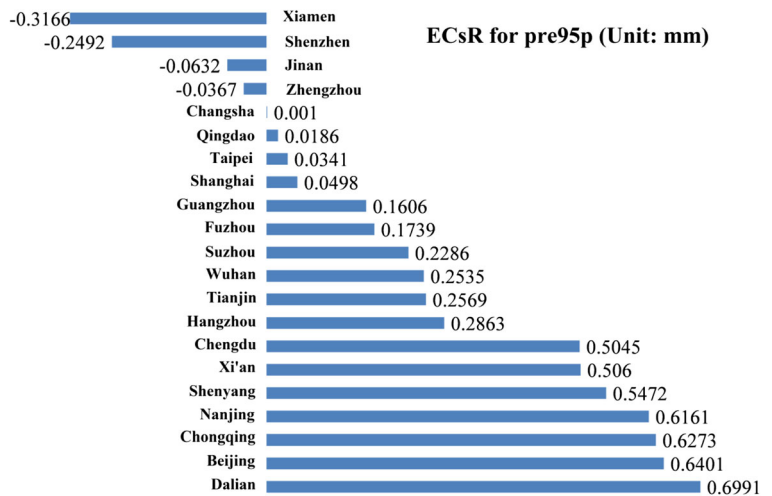
Accuracy analysis of TMPA data

As the direct measurement, gauges provide the most reliable estimate of precipitation (Kidd and Huffman 2011), but at the point scale. In addition, rain gauges are always limited due to their uneven distribution, which becomes particularly problematic when different interpolation methods are used to obtain continuous spatial precipitation estimates and gridded data. In order to derive the extreme rainfall at the area scale, the

version 7 TMPA 3B42 products were used in this study. The products have higher accuracy in urban areas because about 600–700 rainfall gauges in China that are located around some cities were used to correct the rainfall products (Schneider et al. 2014). In the 21 typical cities, 19 have 19 rainfall gauges for TRMM correction,⁵ respectively located in Beijing, Tianjin, Shenyang, Dalian, Jinan, Qingdao, Zhengzhou, Xi'an, Chengdu, Chongqing, Changsha, Wuhan, Nanjing, Shanghai, Hangzhou, Guangzhou, Shenzhen, Xiamen, and Fuzhou. Additionally, Suzhou is close to Shanghai and Nanjing; Taipei is close to Xiamen. Some studies

⁵ <https://www.ncdc.noaa.gov>

Fig. 9 ECsR for pre95p in the 21 typical urban areas



also proved that TMPA products in these regions have higher accuracy compared with rainfall gauges (Chen et al. 2013; Shen et al. 2010; Li et al. 2017a, b).

In the abovementioned 19 rainfall gauges, there are 4 rain gauges' missing parts of rainfall records during 1998–2015. Furthermore, we selected the whole daily rainfall data from the remaining 15 rainfall gauges, to compare with TMPA 3B42 products. The daily rainfall data from 15 rain gauges during 1998–2015 were collected from China Metrological Data Service Center (<http://data.cma.cn/en>).⁶ Figure 8 shows the values of trends in pre95p and pre99p extreme rainfalls based on TMPA against rain gauges; it also could be seen that the trends in pre95p ($R^2 = 0.9541$) and pre99p ($R^2 = 0.9418$) extreme rainfalls by TMPA 3B42 have high correlation with rain gauges. In Fig. 8, X' is the value of trend calculated from rain gauge, and X is that calculated from TMPA 3B42. Totally, most values of the trends from the former are greater than those from the latter.

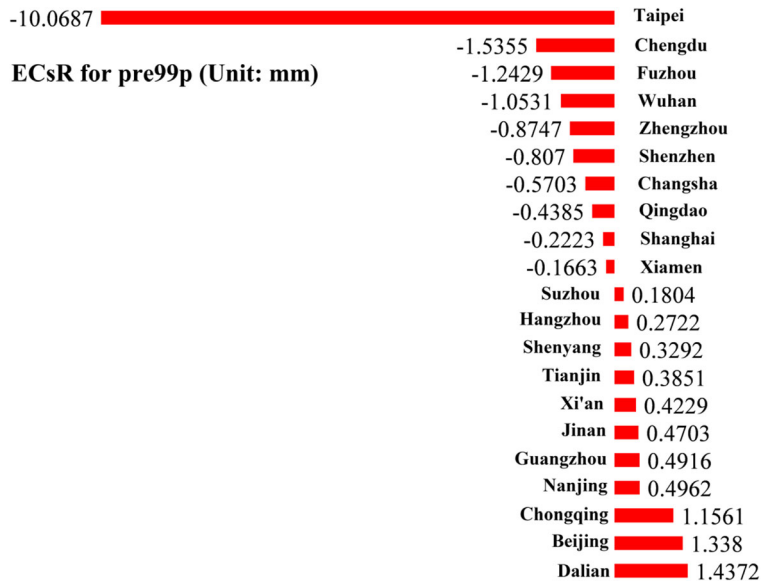
Discussion

In this study, extreme rainfall was analyzed for 21 typical urban areas of China based on remotely sensed data including TMPA 3B42 and MCD12Q1 products. Considering two parameters—pre95p and pre99p, we examined the trends of extreme rainfall from 1998 to

2015. In the 21 typical urban areas grouped into four climatic zones, more than half show an increase tendency in the daily occurrence of extreme rainfall from 1998 to 2015. Figures 9 and 10 show ECsR for pre95p and pre99p in the 21 urban areas. These urban areas are ranked by the value of the ECsR from the smallest negative one to the largest positive value. When the value of ECsR is greater than 0, it reveals an upward trend of extreme rainfall; otherwise, it reveals a downward trend. When the value is equal to 0, the trend is steady with little change. The higher the value of $|a|$ is, the faster the trends of change. In the 21 urban areas, 17 have upward trends of pre95p extreme rainfall; 11 have upward trends of pre99p extreme rainfall. The Dalian urban area has the fastest upward pre95p and pre99p extreme rainfall. Inversely, the fastest downward trend of pre95p extreme rainfall occurred in the Xiamen. It is worth noted that Taipei has the fastest downward trend of pre99p extreme rainfall that has been estimated to reduce about 10 mm from 1998 to 2015. Additionally, Changsha has a relative small change rate of pre95p extreme rainfall.

During the period 1998–2015, many cities had a rapid urban expansion in China. Rapid urbanization has brought about increasing urban heat island effect due to a drastic sprawl of concrete buildings and city infrastructures, which are important factors influencing extreme precipitation (Deng et al. 2018). Song et al. (2014) showed urban areas of Beijing had a significantly higher growth rate after 2000 and found that the trend in annual precipitation is more evident with a linear variation of 12.213 mm per year. In our study, we found that Beijing exhibit an upward extreme rainfall tendency in

⁶ <http://data.cma.cn/en>

Fig. 10 ECsR for pre99p in the 21 typical urban areas

this period. Especially in 2012, the 99th threshold reached approximately 140 mm/day. Liang and Ding (2017) found that changes in the frequency and total intensity of heavy precipitation indicate significant increasing trends in urban and suburban areas from 1981 to 2014. In our study, the urban areas of Shanghai have increasing trends in the 95th extreme precipitation and the highest value for pre99p extreme rainfall larger than 140 mm/day in Yangtze River Delta. Lu et al. (2019) found that urban expansion could increase the magnitudes of extreme precipitation and its recurrence levels in Yangtze River Delta. In our study, three urban areas (e.g., Nanjing, Suzhou, and Hangzhou) of Yangtze River Delta exhibit obvious upward tendencies in extreme rainfall during 1998–2015.

Conclusions

Major conclusions of this study can be summarized as follows:

1. More than 66% (50%) of the regions of China covered by TMPA 3B42 have increasing trends (i.e., NI, HI, and VHI) in pre95p (pre99p) extreme precipitation.
2. In the 21 typical urban areas, over half exhibit upward tendencies of extreme rainfall, especially for pre95p, and 17 have upward trends of extreme rainfall including Shanghai, Nanjing, and Suzhou in

the Yangtze River Delta region. It is noted that Dalian urban areas have the fastest increasing trends in pre95p and pre99p extreme rainfall. The results also illustrate that southeastern coastal urban areas of China may have experienced decreasing occurrences in extreme rainfall.

In future research, we will evaluate rainfall data from more sources such as higher-resolution gridded precipitation data and Weather Research Forecasting (WRF), combined with climate models to explore the relationship between extreme rainfall and the process of urbanization.

Funding information This work was supported by the National Natural Science Foundation of China (Grant Nos. 41501458 and 41730642), the Natural Science Foundation of Shanghai (Grant No. 19ZR1437500), the National Key Research and Development Program of China (No. 2016YFC0502706), open fund of Shandong Provincial Key Laboratory of Water and Soil Conservation and Environmental Protection (STKF201902), and the Shanghai Gaofeng & Gaoyuan Project for University Academic Program Development.

References

- Aalst, M. K. V. (2006). The impacts of climate change on the risk of natural disasters. *Disasters*, 30(1), 5–18.
- Ackerman, A., Kirkpatrick, M., Stevens, D., & Toon, O. (2004). The impact of humidity above stratiform clouds on indirect aerosol climate forcing. *Nature*, 432(7020), 1014–1017.

- Agarwal, M., & Tandon, A. (2010). Modeling of the urban heat island in the form of mesoscale wind and of its effect on air pollution dispersal. *Applied Mathematical Modelling*, 34(9), 2520–2530.
- Alexander, L. V., Zhang, X., Peterson, T. C., Caesar, J., Gleason, B., Klein Tank, A. M. G., Haylock, M., Collins, D., Trewin, B., Rahimzadeh, F., Taghipour, A., Rupa Kumar, K., Revadekar, J., Griffiths, G., Vincent, L., Stephenson, D. B., Burn, J., Aguilar, E., Taylor, M., New, M., Zhai, P., Rusticucci, M., & Vazquez-Aguirre, J. L. (2012). Global observed changes in daily climate extremes of temperature and precipitation. *Journal of Geophysical Research-Atmospheres*, 111(D5), 1042–1063.
- Allan, R. P., & Soden, B. J. (2008). Atmospheric warming and the amplification of precipitation extremes. *Science*, 321(5895), 1481–1484.
- Barredo, J. I. (2007). Major flood disasters in Europe: 1950–2005. *Natural Hazards*, 42(1), 125–148.
- Cetin, M. (2015a). Determining the bioclimatic comfort in Kastamonu city. *Environmental Monitoring and Assessment*, 187(10), 640.
- Cetin, M. (2015b). Using GIS analysis to assess urban green space in terms of accessibility: case study in Kutahya. *International Journal of Sustainable Development and World Ecology*, 22(5), 420–424.
- Cetin, M. (2016). Sustainability of urban coastal area management: a case study on Cide. *Journal of Sustainable Forestry*, 35(7), 527–541.
- Cetin, M., & Sevik, H. (2016). Evaluating the recreation potential of Ilgaz Mountain National Park in Turkey. *Environmental Monitoring and Assessment*, 188(1), 52.
- Cetin, M., Adiguzel, F., Kaya, O., & Sahap, A. (2018). Mapping of bioclimatic comfort for potential planning using GIS in Aydin. *Environment, Development and Sustainability*, 20(1), 361–375.
- Chen, S., Hong, Y., Cao, Q., Kirstetter, P., Gourley, J. J., Qi, Y., Zhang, J., Howard, K., Hu, J., & Wang, J. (2013). Performance evaluation of radar and satellite rainfalls for Typhoon Morakot over Taiwan: are remote-sensing products ready for gauge denial scenario of extreme events? *Journal of Hydrology*, 506, 4–13.
- Chen, Z., Yin, L., Chen, X., Wei, S., & Zhu, Z. (2016). Research on the characteristics of urban rainstorm pattern in the humid area of Southern China: a case study of Guangzhou city. *International Journal of Climatology*, 35(14), 4370–4386.
- Chou, C., Chen, C. A., Tan, P. H., & Chen, K. T. (2012). Mechanisms for global warming impacts on precipitation frequency and intensity. *Journal of Climate*, 25(9), 3291–3306.
- Deng, Y., Jiang, W., He, B., Chen, Z., & Jia, K. (2018). Change in Intensity and frequency of extreme precipitation and its possible teleconnection with large-scale climate index over the China from 1960 to 2015. *Journal of Geophysical Research-Atmospheres*, 123(4), 2068–2081.
- Domrös, M., & Peng, G. (2012). *The climate of China*. Berlin: Springer.
- Donat, M. G., Lowry, A. L., Alexander, L. V., O’Gorman, P. A., & Maher, N. (2016). More extreme precipitation in the world’s dry and wet regions. *Nature Climate Change*, 6(5), 508–514.
- Frich, P., Alexander, L. V., Della-Marta, P. M., Gleason, B., Haylock, M., Klein Tank, A. M. G., & Peterson, T. (2002). Observed coherent changes in climatic extremes during the second half of the twentieth century. *Climate Research*, 19(3), 193–212.
- Georgescu, M., Morefield, P. E., Bierwagen, B. G., & Weaver, C. P. (2014). Urban adaptation can roll back warming of emerging megapolitan regions. *Proceedings of the National Academy of Sciences*, 111(8), 2909–2914.
- Han, J. Y., Baik, J. J., & Lee, H. (2014). Urban impacts on precipitation. *Asia-Pacific Journal of Atmospheric Sciences*, 50(1), 17–30.
- Hu, C., Xu, Y., Han, L., Yang, L., & Xu, G. (2016). Long-term trends in daily precipitation over the Yangtze River delta region during 1960–2012, Eastern China. *Theoretical and Applied Climatology*, 125(1–2), 131–147.
- Huang, D., Zhang, T., & Zhou, F. (2010). Sea-surface temperature fronts in the Yellow and East China Seas from TRMM microwave imager data. *Deep Sea Research Part II: Topical Studies in Oceanography*, 57(11), 1017–1024.
- Huang, Y., Chen, S., Cao, Q., Hong, Y., Wu, B., Huang, M., Qiao, L., Zhang, Z., Li, Z., Li, W., & Yang, X. (2013). Evaluation of version-7 TRMM multi-satellite precipitation analysis product during the Beijing extreme heavy rainfall event of 21 July 2012. *Water*, 6(1), 32–44.
- Huffman, G. J., Bolvin, D. T., Nelkin, E. J., Wolff, D. B., Alder, R. F., Gu, G., Hong, Y., Bowman, K. P., & Stocker, E. F. (2007). The TRMM multisatellite precipitation analysis (TMPA): Quasi-global, multiyear, combined-sensor precipitation estimates at fine scales. *Journal of Hydrometeorology*, 8, 38–55.
- IPCC (Intergovernmental Panel on Climate Change). (2013). Summary for policymakers. In *Climate change 2013: the physical science basis*. In T. F. Stocker, D. Qin, G.-K. Plattner, M. Tignor, S. K. Allen, J. Boschung, A. Nauels, Y. Xia, V. Bex, & P. M. Midgley (Eds.), *Contribution of Working Group I to the fifth assessment report of the Intergovernmental Panel on Climate Change*. Cambridge: Cambridge University Press.
- Jia, S., Zhu, W., Lü, A., & Yan, T. (2011). A statistical spatial downscaling algorithm of TRMM precipitation based on NDVI and DEM in the Qaidam Basin of China. *Remote Sensing of Environment*, 115(12), 3069–3079.
- Joyce, R. J., Janowiak, J. E., Arkin, P. A., & Xie, P. (2004). CMORPH: A method that produces global precipitation estimates from passive microwave and infrared data at high spatial and temporal resolution. *Journal of Hydrometeorology*, 5, 487–503.
- Kaya, L. G., Kaynakci-Elinc, Z., Yucedag, C., & Cetin, M. (2018). Environmental outdoor plant preferences: a practical approach for choosing outdoor plants in urban or suburban residential areas in Antalya, Turkey. *Fresenius Environmental Bulletin*, 27(12), 7945–7952.
- Kidd, C., & Huffman, G. (2011). Global precipitation measurement. *Meteorological Applications*, 18(3), 334–353.
- Li, D., Chistakos, G., Ding, X., & Wu, J. (2017a). Adequacy of TRMM satellite rainfall data in driving the SWAT modeling of Tiaoxi catchment (Taihu lake basin, China). *Journal of Hydrology*, 556, 1139–1152.
- Li, W., Liu, C., Scaioni, M., Sun, W., Chen, Y., Yao, D., Chen, S., Hong, Y., Zhang, K., & Cheng, G. (2017b). Spatio-temporal analysis and simulation on shallow rainfall-induced landslides in China using landslide susceptibility dynamics and

- rainfall ID thresholds. *Science China Earth Sciences*, 60(4), 720–732.
- Liang, P., & Ding, Y. (2017). The long-term variation of extreme heavy precipitation and its link to urbanization effects in Shanghai during 1916–2014. *Advances in Atmospheric Sciences*, 34(3), 321–334.
- Liang, P., Ding, Y. H., He, J. H., & Tang, X. (2013). Study of relationship between urbanization speed and change in spatial distribution of rainfall over Shanghai. *Journal of Tropical Meteorology*, 19, 97–103.
- Libertino, A., Sharma, A., Lakshmi, V., & Claps, P. (2016). A global assessment of the timing of extreme rainfall from TRMM and GPM for improving hydrologic design. *Environmental Research Letters*, 2016, 11(5).
- Lu, M., Xu, Y., Shan, N., Wang, Q. (2019). Effect of urbanisation on extreme precipitation based on nonstationary models in the Yangtze River Delta metropolitan region. *Science of The Total Environment*, 673, 64–73.
- Meehl, G. A., Arblaster, J. M., & Tebaldi, C. (2005). Understanding future patterns of increased precipitation intensity in climate model simulations. *Geophysical Research Letters*, 32(18), 109–127.
- O’Gorman, P. A. (2015). Precipitation extremes under climate change. *Current Climate Change Reports*, 1(2), 49–59.
- Olson, W. S., Kummerow, C. D., Heymsfield, G. M., & Giglio, L. (1996). A method for combined passive-active microwave retrievals of cloud and precipitation profiles. *Journal of Applied Meteorology*, 35(10), 1763–1789.
- Pendergrass, A. G., & Knutti, R. (2018). The uneven nature of daily precipitation and its change. *Geophysical Research Letters*, 45(21), 11,980–11,988.
- Pfeifer, M., Disney, M., Quaipe, T., & Marchant, R. (2011). Terrestrial ecosystems from space: a review of earth observation products for macroecology applications. *Global Ecology and Biogeography*, 21(6), 603–624.
- Qian, W. H., & Lin, X. (2005). Regional trends in recent precipitation indices in China. *Meteorology and Atmospheric Physics*, 90(3–4), 193–207.
- Quan, R. (2014). Risk assessment of flood disaster in Shanghai based on spatial-temporal characteristics analysis from 251 to 2000. *Environmental Earth Sciences*, 72(11), 4627–4638.
- Rajasekar, U., & Weng, Q. (2009). Urban heat island monitoring and analysis using a non-parametric model: a case study of Indianapolis. *ISPRS Journal of Photogrammetry and Remote Sensing*, 64(1), 86–96.
- Schneider, U., Becker, A., Finger, P., Meyer-Christoffer, A., Ziese, M., & Rudolf, B. (2014). GPCC’s new land surface precipitation climatology based on quality-controlled in situ data and its role in quantifying the global water cycle. *Theoretical and Applied Climatology*, 115(1–2), 15–40.
- Shen, Y., Xiong, A., Wang, Y., & Xie, P. (2010). Performance of high-resolution satellite precipitation products over china. *Journal of Geophysical Research-Atmospheres*, 115(D2), 355–365.
- Song, X., Zhang, J., AghaKouchak, A., Roy, S. S., Xuan, Y., Wang, G., He, R., Wang, X., & Liu, C. (2014). Rapid urbanization and changes in spatiotemporal characteristics of precipitation in Beijing metropolitan area. *Journal of Geophysical Research-Atmospheres*, 119(19), 11,250–11,271.
- Sorooshian, S., Hsu, K. L., Gao, X., Gupta, H. V., Imam, B., & Dan, B. (2000). Evaluation of PERSIANN system satellite-based estimates of tropical rainfall. *Bulletin of the American Meteorological Society*, 81, 2035–2046.
- Tang, Q., Zhang, X., & Francis, J. A. (2014). Extreme summer weather in northern mid-latitudes linked to a vanishing cryosphere. *Nature Climate Change*, 4(1), 45–50.
- Tarnavsky, E., Mulligan, M., Ouessar, M., Faye, A., & Black, E. (2013). Dynamic hydrological modeling in drylands with TRMM based rainfall. *Remote Sensing*, 5(12), 6691–6716.
- Tebaldi, C. A., & Knutti, R. (2007). The use of the multi-model ensemble in probabilistic climate projections. *Philosophical Transactions of the Royal Society A - Mathematical Physical and Engineering Sciences*, 365(1857), 2053–2075.
- Wang, Y., & Yan, Z. W. (2009). Trends in seasonal precipitation over china during 1961–2007. *Atmospheric & Oceanic Science Letters*, 2(3), 165–171.
- Wang, K., Wang, L., Wei, Y. M., & Ye, M. (2013). Beijing storm of July 21, 2012: observations and reflections. *Natural Hazards*, 67(2), 969.
- Wu, Y., Wu, S. Y., Wen, J., Xu, M., & Tan, J. (2015). Changing characteristics of precipitation in China during 1960–2012. *International Journal of Climatology*, 36(3), 1387–1402.
- Xu, W., Zipser, E. J., & Liu, C. (2009). Rainfall characteristics and convective properties of mei-yu precipitation systems over South China, Taiwan, and the South China Sea. Part I: TRMM observations. *Monthly Weather Review*, 137(12), 4261–4275.
- Yang, X. (2013). China’s rapid urbanization. *Science*, 342(6156), 310–310.
- Yang, L., Scheffran, J., Qin, H., & You, Q. (2015). Climate-related flood risks and urban responses in the Pearl River Delta, China. *Regional Environmental Change*, 15(2), 379–391.
- Yucedag, C., Kaya, L. G., & Cetin, M. (2018). Identifying and assessing environmental awareness of hotel and restaurant employees’ attitudes in the Amasra District of Bartin. *Environmental Monitoring and Assessment*, 190(2), 60.
- Zeng, J., Chen, K. S., Bi, H., & Chen, Q. (2016). A preliminary evaluation of the SMAP radiometer soil moisture product over United States and Europe using ground-based measurements. *IEEE Transactions on Geoscience and Remote Sensing*, 54(8), 4929–4940.
- Zhai, P., Sun, A., Ren, F., Liu, X., Gao, B., & Zhang, Q. (1999). Changes of climate extremes in China. *Climate Change*, 42(1), 203–218.
- Zhai, P., Zhang, X., Wan, H., & Pan, X. (2005). Trends in total precipitation and frequency of daily precipitation extremes over china. *Journal of Climate*, 18(7), 1096–1108.
- Zhang, G., Biradar, C. M., Xiao, X., Dong, J., Zhou, Y., Qin, Y., Zhang, Y., Liu, F., Ding, M., & Thomas, R. (2018). Exacerbated grassland degradation and desertification in Central Asia during 2000–2014. *Ecological Applications*, 28(2), 442–456.

Publisher’s note Springer Nature remains neutral with regard to jurisdictional claims in published maps and institutional affiliations.